Laser structuring of thin-film solar cells on polymers

P. Gečys, G. Račiukaitis, M. Gedvilas, A. Selskis

Laser Structuring of Thin-Film Solar Cells on Polymers

P.Gečys[1], G.Račiukaitis[1a], M.Gedvilas[1] and A.Selskis[2]

[1]Laboratory for Applied Research, Institute of Physics, Savanoriu Ave. 231, LT-02300 Vilnius, Lithuania
[2]Institute of Chemistry, A. Goštauto 9, LT-01108 Vilnius, Lithuania

Abstract. A permanent growth of the thin-film electronics market stimulates the development of versatile technologies for patterning thin-film materials on flexible substrates. High repetition rate lasers with a short pulse duration offer new possibilities for high efficiency structuring of conducting, semi-conducting and isolating films. Lasers with the picosecond pulse duration were applied in structuring the complex multilayered Cu(InGa)Se_2 (CIGS) solar cells deposited on the polyimide substrate. The wavelength of laser radiation was adjusted depending on optical properties both of the film and the substrate. A narrow processing window of laser fluence and pulse overlap was estimated with both 1064 nm and 355 nm irradiation to remove the molybdenum backcontact off the substrate. The selective removal of ITO, ZnO and CIGS layers was achieved with 355 nm irradiation in the multilayer structure of CIGS without significant damage to the underneath layers. Use of the flat-top laser beam profile should prevent inhomogeneity in ablation. The EDS analysis did not show residues of molybdenum projected onto the walls of ablated channel due to melt extrusion. Processing with picosecond lasers should not cause degradation of photo-electrical properties of the solar cells but verification is required.

PACS. 42.62.Cf Industrial laser applications - 81.40.Wx Radiation treatment - 81.05.Hd Other semiconductors - 89.30.Cc Solar power - 68.65.Ac Multilayers - 68.37.Hk Scanning electron microscopy

[a] e-mail: graciukaitis@ar.fi.lt

1 Introduction

A permanent growth of the thin-film electronics market stimulates the development of versatile technologies for patterning thin-film materials on rigid and flexible substrates. Utilization of laser radiation provides diversity of processing means for structuring deposited films. Interest in complex multilayered Cu(InGa)Se_2 (CIGS) solar cells has increased recently because of low production costs [1]. Efficiency of the thin-film solar cells with a large active area might be increased if small segments are connected in series in order to reduce photocurrent in thin films and resistance losses. Selective removal of the films in multilayer structures of modern Solar cells is crucial for performance of the devices. Lasers are usually used to scribe the separation lines for isolation and element contacts by selective ablation of conducting and semi-conducting layers. Accuracy in the ablation depth and a high scribing speed are required for efficient and cost-effective production of Solar cells of this type. High repetition rate lasers with a short pulse duration offer new possibilities for high efficiency structuring of conducting, semi-conducting and isolating films. Various laser sources were tested in selective ablation of thin films [2-6]. The main limiting factor for laser processing of the multilayer $CuInSe_2$ structures is deposition of molybdenum on walls of channels scribed in the films, and the phase transition of semi-conducting $CuInSe_2$ to metallic state close to the ablation area due to the thermal effect [4]. Both effects shunt the photo-electric device and decrease its conversion efficiency. Thermal degradation of the CIGS solar cells starts at temperatures above 350^{o}C due to diffusion of the buffer layer metal (Cd, Zn) into the absorber layer [7]. Use of nanosecond lasers is related with a large heat affected zone and nanosecond lasers are undesirable in manufacturing of this type of photovoltaic elements. Femtosecond pulses are capable of ablating the films completely and selectively enough but their use is limited because of complexity in maintenance. According to the results of theoretical modeling, the processing without damage is possible with picosecond laser pulses [5].

Our goal is to develop the flexible and rapid laser technology for precise structuring of the CIGS solar cells compatible with the roll-to-roll production line. We used the laser with the picosecond pulse duration in shaping the simple thin-films structures deposited on glass [8,9] and polymer substrates [10]. They revealed potential of picosecond lasers in selective structuring of thin films when the wavelength of laser radiation was adjusted depending on optical properties both of the film and the substrate. We present our new results in application of laser structuring of multilayered CIGS Solar cells.

2 Samples and Experimental procedures

The films of metals and the whole structure of the CIGS solar cell deposited on the polymer substrates were used in the experiments. Polyimide (PI) film with the thickness of 25 µm was used as a substrate for deposition of molybdenum (0.5 µm) and the complete multilayer structure of Mo/$CuIn_xGa_{(1-x)}Se_2$/CdS/ZnO/ITO. The thickness of the films was 0.5 µm for the Mo back-contact, 1 µm for $CuIn_xGa_{(1-x)}Se_2$ absorber layer, ~10 nm for both CdS and ZnO buffer layers each and 0.5 µm for the top contact of the indium-tin oxide (ITO). All samples on polymer substrates were provided by Solarion AG, Germany.

Set-up for the laser processing experiments included a laser, fast shutter, attenuator, harmonics generation modules, the beam expander, a few folding mirrors, an objective mounted on the Z stage, and the sample mounted on the XY stages. The picosecond laser PL10100 (10 ps, 100 kHz) made by Ekspla UAB was used in the ablation experiments. Nonlinear crystals were used for the wavelength conversion to green and UV radiation. An external Pockels cell was used for fast shuttering and pulse energy control. The beam expander stretched the beam, which was focused with the f = 50 mm focusing lens. Positioning of the samples under the laser beam was performed with the XY stages Aerotech ALS1000. Experimental set-up for laser structuring of the films is shown in Fig. 1.

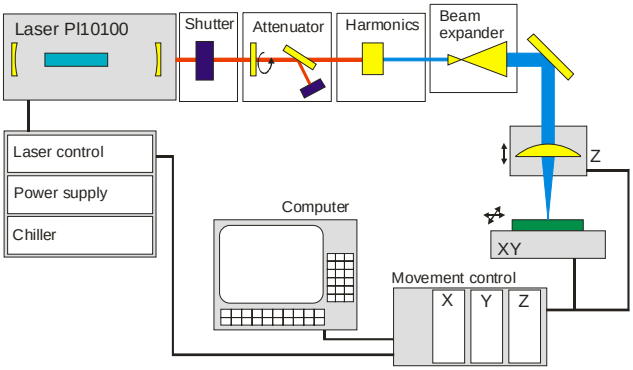

Fig. 1. Experimental set-up for laser structuring of the thin films.

The laser spot overlap along a scanning line was controlled by the translation speed at a constant pulse repetition rate. Various combinations of pulse energy, beam overlap and wavelength were used for etching the films. Optimal regimes for laser processing were estimated depending on the wavelength (1064 nm, 355 nm). The beam overlap played an important role in the processing selectivity because the ablation threshold was sensitive to accumulation of the irradiation dose. The laser processing parameters for selective removal of every layer were estimated.

The quality of processing was evaluated with an optical microscope and atomic force microscope (AFM) CP-II (Veeco). Profiles of the laser ablated holes and trenches and chemical composition of the resulting surfaces were controlled with the scanning electron microscope (SEM) EVO 50 XVP (Zeiss) with the X-ray energy dispersion spectrometer (EDS).

3 Results

3.1 Estimation of the energy density for selective film removal

Thin films for solar cells are deposited over the whole surface homogeneously. Lasers are applied during the production cycle to divide the area into segments for series connections: isolation trenches and contact expositions. Selective evaporation of single layers in multilayer structures is easiest to achieve when resistance of each layer to laser radiation increases from the most top layer to the substrate. In reality, the situation might be opposite when metal films are deposited on soft polymer substrates. Estimation of a proper working window in process parameters is the main task of the technology development.

Series of samples were prepared by ablating craters and trenches in the thin films with picosecond lasers, varying the wavelength of radiation (1064 nm, 355 nm). In case of 1064 nm wavelength, craters were made with a single laser pulse or burst of pulses, consisting of 10, 100 or 1000. Experiments were repeated at least 10 times, and laser pulse energy was changed between series of experiments. When energy density ((fluence) exceeded a certain value depending on material properties, material was evaporated and removed. Experiments were performed on the molybdenum film and the polyimide substrate. The diameter of craters etched by laser radiation was measured and used to estimate the minimal laser fluence that corresponds to the beginning of material evaporation. We used a standard method to estimate the threshold [11]. The results of evaluations are shown in Table 1.

Table 1. Single pulse and multi-pulse (10, 100, 1000) ablation thresholds of molybdenum film and polyimide. Laser: PL10100, 10 ps, 1064 nm. Numbers 1, 10, 100, 1000 are for the number of laser pulses to ablate a crater.

	Ablation threshold F_{th}, J/cm^2			
	1	10	100	1000
Molybdenum	-	5.89	0.9	0.14
Polyimide	1.59	-	0.44	0.13

We did not succeed in initiating ablation of the molybdenum film with a single laser pulse in the range of pulse energies we used. When the film of molybdenum was irradiated by a burst of laser pulses, every pulse modified the surface and the film increasing its absorbtivity. Therefore, the ablation threshold fellt down with an increase of the number of pulses applied to irradiation. The variation can be expressed by an accumulation parameter [12] with a typical value for bulk metals of $\xi = 0.9\text{-}0.7$. Evaluation of the accumulation parameter was performed for the molybdenum film and polyimide. Results are shown in Fig. 2. Our value for the molybdenum film is quite low ($\xi = 0.19$), probably because of limited heat dissipation in the thin film.

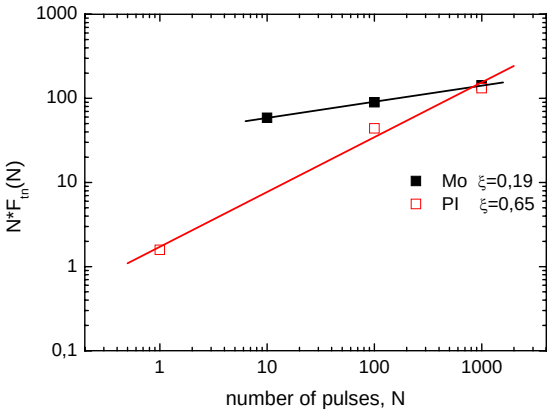

Fig.2. Relation between the number of laser pulses N used to ablate a crater and the multi-pulse ablation threshold of molybdenum film and the polyimide substrate.

Polyimide experienced less variation in its absorption properties. Its ablation threshold also fell down with a number of laser pulses applied, but the effect was less prominent. Ablation properties of both materials became closer in the multi-pulse regime, making selective removal more complicated. Therefore, we limited overlap of laser pulses in the scribing regime when trenches were produced in the films.

3.2 Formation of the Molybdenum backcontact

When the CIGS solar cells are formed on polymer substrates, they are prepared to be illuminated from the top of the CIGS structure. The backcontact is made of the metal film, preferable molybdenum, directly deposited on the substrate. Structuring of the backcontact should be the first laser process in a production line. A homogeneous film of the metal is divided into stripes by local removal of the film and forming isolation trenches in it. Good isolation between the nearby contact lines and the diminishing effect on the substrate are the main requirements at this stage.

As the ablation thresholds of molybdenum and polyimide were close to each other at high beam overlap, we limited the experiments to a high translation speed when only a few laser pulses affected the same area of the film. Moreover, a high processing speed is preferable for the application. Using the infrared 1064 nm laser radiation, the molybdenum film was removed from the substrate. The metal was not evaporated but formed ridges from melt on rims of the processed trench (Fig. 3a). The substrate was damaged when the translation speed was below 600 mm/s at the 50 kHz pulse repetition rate. At a translation speed higher than 700 mm/s, the beam overlap was too small to remove completely the metal along the trench. As the Gaussian spatial profile of the laser beam was used in experiments, central part of the laser spot tended to penetrate into polyimide. Flattening of the profile should help to remove the layer smoothly.

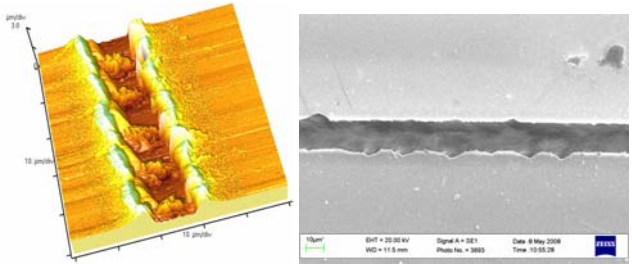

a) b)

Fig.3. Pictures of trenches ablated with a laser: a) AFM picture (laser: λ=1064 nm, 2.4 W, 50 kHz, translation speed 600 mm/s); b) SEM picture (laser: λ=355 nm, 2.35 W, 100 kHz; translation speed 600 mm/s).

Similar experiments were performed using laser radiation converted to ultraviolet (UV) at the 355 nm wavelength. Removal of the metal film by evaporation from the polymer substrate with a low melting temperature, tended to damage the substrate by the high intensive center of the laser spot. The main difference of the processing quality using the UV radiation was clean edges of trenches without appreciable melt formation (Fig.3b).

3.3 Exposition of the backcontact by removal of the absorber film of complex semiconductor

The semiconducting and solar light absorbing layer of $CuIn_xGa_{(1-x)}Se_2$ deposited on the backcontact should also be structured making parallel trenches in it. We used a complete structure of layers in our experiments instead of a semiproduct to estimate the processing regimes. The goal at this stage was to remove all the top layers, including CIGS and to expose the molybdenum backcontact.

The first experiments included ablation of craters with 10 laser pulses with different pulse energies in series. Ten pulses corresponded to the value of the laser beam overlap when quality of trenches was the best without significant damage of the polyimide substrate in previous experiments. Fig.4. shows SEM pictures of craters made at three different pulse energies. The 20 μJ pulse energy was apparently too high, because the laser beam penetrated the Mo layer and damaged the substrate.

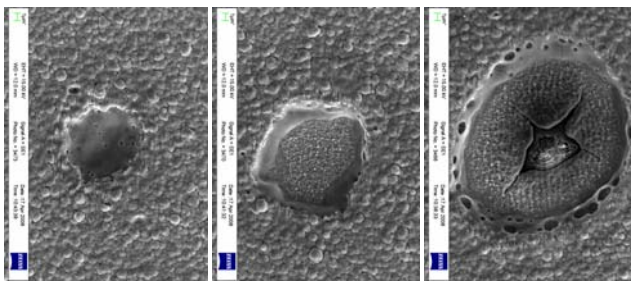

3.5 μJ 5 μJ 20 μJ

Fig.4. SEM pictures of craters made with 10 laser pulses in the ITO/Zn0/CdS/$CuIn_xGa_{(1-x)}Se_2$/Mo/PI multilayer (laser: 1064 nm; pulse energies are indicated below the pictures).

All samples were investigated with SEM using the X-ray electron dispersion spectrometer because visual contrast did not

allow discrimination of differences in chemical composition of layers. Fig.5. presents comparison of the SEM pictures with the EDS maps of spatial distribution of separate chemical elements in a close surrounding of the laser made craters.

By ablating with pulse energy of 3.5 μJ, concentration of In decreased and a signal from Se atoms appeared in the center of the crater. The top layer of conducting ITO/ZnO was evaporated and CIGS layer was exposed. Use of higher pulse energy (5 μJ) exposed the CIGS layer in a larger area but in the center part of the crater, where laser intensity was higher, the whole material was evaporated and molybdenum backcontact was exposed. At the pulse energy of 20 μJ, carbon atoms from the polymer were found in EDS spectra.

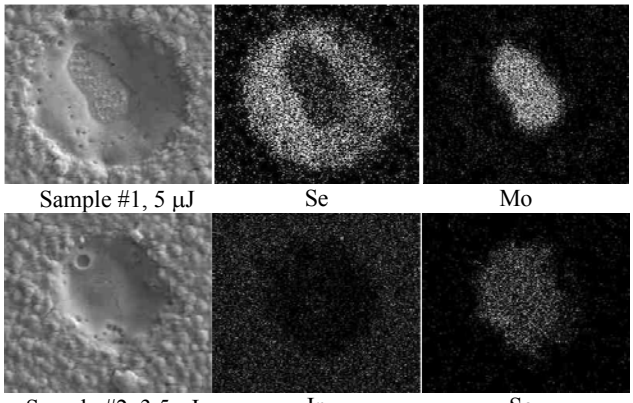

Fig.5. SEM pictures and EDS maps of the craters ablated with 10 laser pulses with the energy of 5 μJ and 3.5 μJ. (laser: λ=1064 nm).

The UV laser radiation (355 nm) was also applied at this stage of investigations. It was used to ablate selectively trenches in layers of the CIGS solar cell structure. We estimated the following regimes for selective removal of films:

- to evaporate the upper electro-conducting layer of ITO;
- to remove the semiconducting film and expose the molybdenum backcontact;
- to make an isolation trench by laser ablation of all films down tol the polyimide substrate;
- to cut a complete structure of the CIGS solar cell together with the substrate.

The process parameters of the regimes are presented in Table 2.

Table 2. Regimes of selective removal of layers and cutting the CIGS multilayer structure in solar cell formation. (Laser PL10100: P= 2.35 W, λ=355 nm, 100 kHz).

Regime	Scanning speed, mm/s	Process
#1	900	Removal of the ITO film
#2	380	Exposition of the Mo back-contact
#3	150	Isolation trench until polyimide
#4	35	Cutting of the CIGS multilayer

SEM pictures of trenches ablated in CIGS structure at different regimes (Table 2) and distribution of main chemical components in the cross-section of trenches are shown in Fig.6. The top layer of ITO and thin buffer layers of ZnO and CdS were removed at regime #1 cleanly (Fig.6a). The Se and Cu signals were detected with the EDS at the bottom of trench with a synchronous decrease in the concentration of In. Those elements construct the absorber layer. Molybdenum and carbon were found at the background level.

The 355 nm radiation was badly absorbed by ITO and thermal exfoliation prevailed [8]. The surface of the CIGS layer shows some marks of melting in the central part of the trench. As the properties of the surface of CIGS strongly depend on the bulk stoichiometry [13], heating might affect electrical properties of CIGS and special experiments are intended.

When the translation speed was reduced to 380 mm/s keeping all other processing parameters the same (Fig. 6b) the laser was able to evaporate CIGS film and expose the Mo backcontact. The high signal of Mo atoms was detected with the EDS in the central part of the trench.

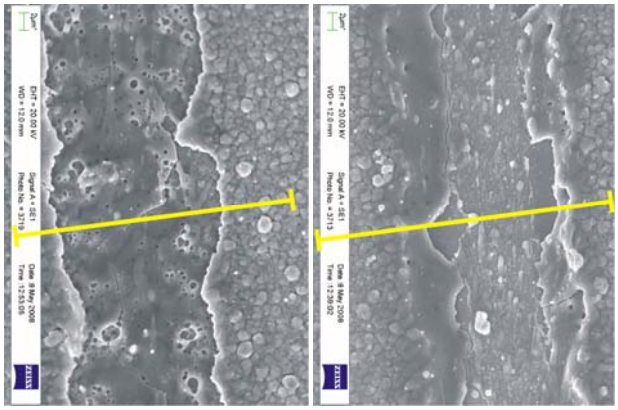

a) b)

Fig.6. SEM picture of a trench ablated in: a) the ITO/ZnO top layer to expose the absorber film (translation speed 900 mm/s); b) down to the Mo layer to expose the backcontact (translation speed 380 mm/s). Laser: 2.35 W, λ=355 nm, 100 kHz.

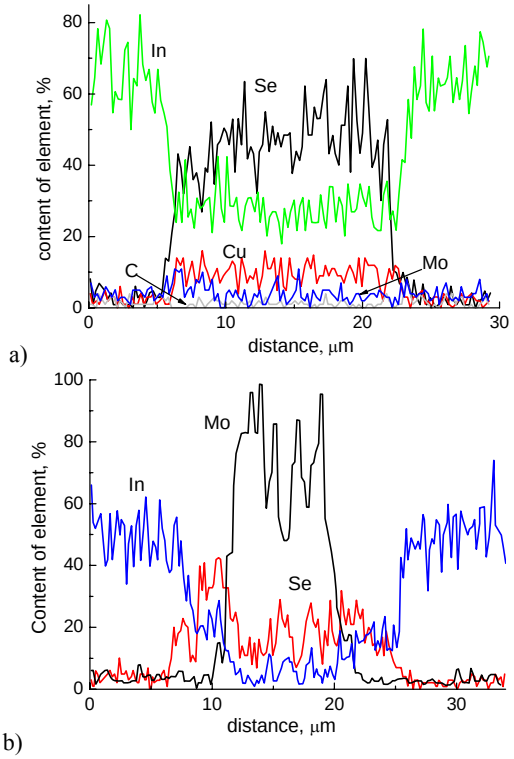

Fig.6. EDS cross-section of a trench ablated in: a) the ITO/ZnO top layer to expose the absorber film (translation speed 900 mm/s); b) down to the Mo layer to expose the backcontact (translation speed 380 mm/s).

The trenches had inclined walls. This is a consequence of the Gaussian spatial distribution of energy in the laser beam. Slopes of the trenches were formed of a partially removed layer and in case of Fig. 6b included $CuIn_xGa_{(1-x)}Se_2$ as quite strong signals of Se were detected with EDS. The trenches were narrow enough to ensure dense dislocation of separation lines between elements in solar cells. The upper layer of the top contact was not affected outside of the irradiation area.

The regime #3 was used to make the edge isolation – to remove completely all the layers from the polyimide substrate. The trenches had sharp edges with only a little penetration into the substrate which had no effect on its mechanical strength. A quite slow translation speed was used to cut the whole CIGS/substrate structure with the picosecond laser. Cuts of this kind are not required in the real production cycle, but the EDS investigations of a cross-section provided information about the quality of laser processing. SEM picture of the cross-section of the multi-layer CIGS structure is shown in Fig.7. Separate layers can be easily recognized in the picture which means that there was no mixing during the deposition cycle and the laser processing did not disturb regular position of the layers with sharp edges. J. Hermann et al. [4] estimated that processing of CIGS solar cells with nanosecond lasers led to spreading of molybdenum over the CIGS film creating short-cuts. The picosecond pulse duration was short enough to prevent extensive formation of melt and no mixing of Mo with CIGS was found. The EDS signals of the main chemical components of CIGS were measured along the cut depth (indicated by arrow in Fig. 7).

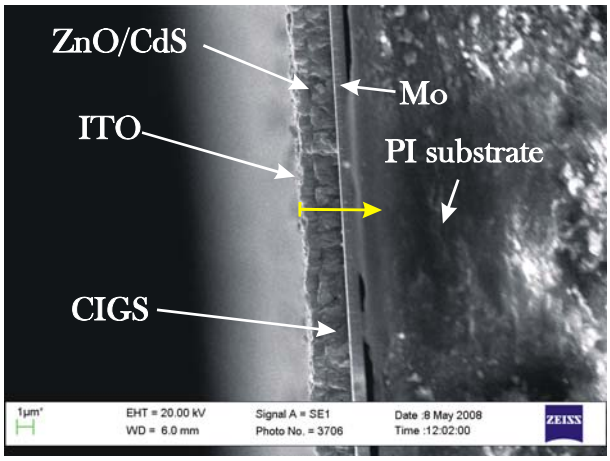

Fig.7. Cross-section of the CIGS photovoltaic element cut with the laser and its chemical composition estimated by EDS. (laser: 2.35 W, λ=355 nm, 100 kHz; translation speed 35 mm/s). Arrow indicates the EDS scan direction. Length of the arrow is 5 µm.

Atoms of molybdenum appeared in EDS spectra on the edge of the Mo layers and were spread toward the polyimide substrate (Fig.8). The rise in Mo concentration was at the same depth where concentrations of In and Cu atoms decreased.

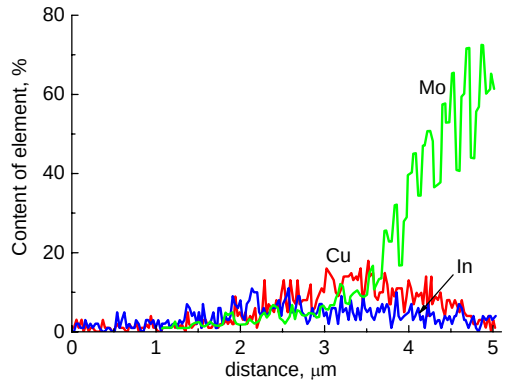

Fig.8. EDS scans of chemical elements, starting with the top layers of the CIGS structure.

4 Conclusions

Laser direct write with the picosecond pulse duration was applied in structuring the thin-films deposited on the polyimide substrate. The wavelength of laser radiation was adjusted depending on optical properties both of the film and the substrate. Absorption of laser radiation by the film material was essential to initiate its controllable removal.

- A narrow processing window of laser fluence and pulse overlap was estimated with both 1064 nm and 355 nm wavelength of laser radiation to remove the molybdenum backcontact off the substrate. The ablation thresholds of Mo and polyimide became closer due to the defect accumulation which increased with the beam overlap.
- The selective removal of ITO, CIGS and Mo layers was achieved with the 355 nm irradiation without significant damage to the underneath layers.
- Scribing the thin film layers with the Gaussian beam profile caused damage in the center of laser machined trench. To avoid damage and increase process productivity it is necessary to convert it to a flat top profile beam.
- The EDS analysis showed no residues of molybdenum projected onto the walls of ablated trench due to melt extrusion. Processing with picosecond lasers should not cause short-cut formation and degradation of photo-electrical properties of the solar cells but verification is required.

The work was supported by the Lithuanian State Science and Studies Foundation under project No B-31/2008. We acknowledge our thanks to Solarion AG, Germany, for kind support with the samples.

References

1. N.G. Dhere, Solar Energy Materials and Solar Cells, **91**, 1376 (2007).
2. R. Tanaka, T. Takaoka, H. Mizukami, T. Arai, Y. Iwai, Proc. SPIE **5063**, 370 (2003).
3. D. Ashkenasi, A. Rosenfeld, *Proc. SPIE* 4637, 169 (2002).
4. J. Hermann, M. Benfarah, et al., J. Phys. D, **39**, 453 (2006).
5. A.D. Compaan, I. Matulionis, S. Nakade, Optics and Lasers Engineering **34, 15** (2000).
6. C. Molpeceres, S. Lauzurica, J.L. Ocana, J.J. Gandia, L. Urbina, J. Carabe, J. Micromech. Microeng. **15**, 1271 (2005).
7. S. Kijima, T. Nakada, Jap. Appl. Phys. Express, **1**, 075002 (2008).
8. G. Račiukaitis, M. Brikas, M. Gedvilas, T. Rakickas, Appl. Surface Science, **253**, 6584 (2007).
9. G. Račiukaitis, M. Brikas, M. Gedvilas, G. Darčianovas, J. Laser Micro/Nanoengineering, **2**(1), 1 (2007).
10. G. Račiukaitis, M. Brikas, G. Darčianovas, D. Ruthe, K. Zimmer, Proc. of SPIE **6732**, 67320C (2007).
11. J.M. Liu, *Opt. Lett.*, **7**, 196 (1982).
12. Y. Jee, M.F. Becker and R.M. Walser, J. Opt. Soc. Am. B, **5**, 648 (1988).
13. A. Rockett, Thin Solid Films **361-2**, 330 (2000).